

## A FAST SPECTRAL SOLVER FOR A 3D HELMHOLTZ EQUATION\*

E. BRAVERMAN<sup>†</sup>, M. ISRAELI<sup>†</sup>, AND A. AVERBUCH<sup>‡</sup>

**Abstract.** We present a fast solver for the Helmholtz equation

$$\Delta u \pm \lambda^2 u = f,$$

in a 3D rectangular box. The method is based on the application of the discrete Fourier transform accompanied by a subtraction technique which allows us to reduce the errors associated with the Gibbs phenomenon and achieve any prescribed rate of convergence. The algorithm requires  $O(N^3 \log N)$  operations, where  $N$  is the number of grid points in each direction. We solve a Dirichlet boundary problem for the Helmholtz equation. We also extend the method to the solution of mixed problems, where Dirichlet boundary conditions are specified on some faces and Neumann boundary conditions are specified on other faces. High-order accuracy is achieved by a comparatively small number of points. For example, for the accuracy of  $10^{-8}$  the resolution of only 16–32 points in each direction is necessary.

**Key words.** fast 3D solver, Helmholtz equation, Fourier method, Dirichlet and mixed boundary conditions

**AMS subject classifications.** 65N35, 65T20, 35J05

**PII.** S1064827598334241

**1. Introduction.** A fast and accurate solution of elliptic equations is often an important step in the process of solving problems of fluid dynamics and in other scientific computing applications. Helmholtz-type equations usually appear in acoustics or electromagnetics and also appear as a result of time discretization of the Navier–Stokes equations [6].

The approach in the present work is based on the technique developed in [2, 3, 5] for the 2D case and generalizes the method for the 3D Laplace equation in [4]. The efficiency (operation count) of an algorithm is especially important for 3D problems where the computational load is heavy.

In assessing efficiency of algorithms we are really interested in the number of operations required to achieve a certain accuracy. A high-order accurate method would achieve a high accuracy with a small number of degrees of freedom. Thus two algorithms having the same operation count in terms of the resolution  $N$  (the number of points in one direction, say) may be very different in terms of the above criterion. The algorithm developed here can achieve in principle any prescribed rate of convergence if the boundary data is sufficiently smooth. Certain singularities can be handled by the analytical procedure. Furthermore, the number of operations is asymptotically small:  $O(\log N)$  per discretization point.

We consider two cases of nonhomogeneous Helmholtz-type equations, including the monotone case

$$(1.1) \quad \Delta u - \lambda^2 u = f$$

---

\*Received by the editors February 17, 1998; accepted for publication (in revised form) May 27, 1998; published electronically July 22, 1999.

<http://www.siam.org/journals/sisc/20-6/33424.html>

<sup>†</sup>Computer Science Department, Technion-Israel Institute of Technology, Haifa 32000, Israel (maelena@cs.technion.ac.il, israeli@cs.technion.ac.il).

<sup>‡</sup>School of Mathematical Sciences, Tel Aviv University, Tel Aviv 69978, Israel (amir@math.tau.ac.il).

and the oscillatory case

$$(1.2) \quad \Delta u + k^2 u = f$$

with Dirichlet or Neumann boundary conditions.

First, a particular solution of the nonhomogeneous equation is obtained; then an auxiliary problem for an appropriate homogeneous equation is solved. The boundary conditions for the auxiliary problem are obtained as the difference between the original boundary conditions and those obtained from the particular solution. If, for example, the particular solution happens to have zero boundary values for the case of a Dirichlet problem, or zero normal derivative (for a Neumann problem), then we solve the homogeneous equation with the original (specified) boundary conditions.

Thus, the algorithm consists of two steps.

*Step 1.* Solving the nonhomogeneous equation (1.1) or (1.2) with some convenient boundary conditions.

*Step 2.* Solving the corresponding homogeneous equation with the boundary conditions as specified above.

The application of the Fourier method has the following advantages when solving the Helmholtz equation:

1. Differential operators are represented in the Fourier basis by diagonal matrices; this fact reduces the operator inversion to a simple division of the Fourier coefficients by the corresponding wave numbers. The cost of this step is  $O(N^3 \log N)$ , where  $N$  is the number of grid points in each one of the three directions ( $N$  is also the number of Fourier harmonics in the related series representation).
2. If the function is infinitely differentiable and periodic, then a Fourier series approximation to  $f$  converges to  $f$  spectrally, i.e., more rapidly than any finite power of  $1/N$ .

Multidimensional Fourier representations can be considered for Cartesian geometries (rectangles in two dimensions and parallelepipeds in three dimensions). However, rapid convergence of the series representation requires the periodic extension of the solution to have a certain number of continuous derivatives. The periodic extension of a nonperiodic function is discontinuous and the corresponding Fourier series converges only as  $1/N$ . This is not better than a first-order finite-difference scheme. The slow convergence is caused by the so-called Gibbs phenomenon. Below we describe two steps of the algorithm and characterize the methods used to avoid the Gibbs phenomenon. The first step addresses the Gibbs phenomenon in the particular solution via extension; the second step uses subtraction to improve the accuracy of the inhomogeneous solver.

1. The function  $f$  in the right-hand side of (1.1) or (1.2) is extended to a larger domain and replaced by a new function which coincides with  $f$  in the original domain, but the periodic extension of the larger domain has a certain number of continuous derivatives [2, 12]. The extension procedure is based on the local Fourier basis method [10, 13] which employs folding functions as described in [1, 11].
2. An auxiliary boundary value problem for the Helmholtz equation is solved to satisfy the original boundary conditions (in the present work we consider principally the Dirichlet boundary conditions). To reduce the effect of the Gibbs phenomenon the subtraction technique used in [4] for the 3D Laplace equation is employed.

The main results of the paper follow.

1. An accurate and efficient algorithm is developed which solves the Dirichlet problem for the homogeneous Helmholtz equation in  $O(N^3 \log N)$  operations.
2. A fast spectral algorithm is constructed also for the nonhomogeneous boundary value problems of (1.1) and (1.2). This algorithm also requires  $O(N^3 \log N)$  operations. It is to be emphasized that for the present algorithm  $N$  is small; an accuracy of  $10^{-7}$  is usually achieved with  $N = 16$  points in each direction.
3. Similar accuracy and convergence rate are obtained also when we extend the method to mixed problems where on some of the faces Dirichlet boundary conditions are specified, while Neumann boundary conditions are specified on other faces.

The paper is organized as follows. Section 2 is concerned with the solution of a homogeneous Helmholtz equation. It contains a description of the subtraction procedure aimed to reduce the Gibbs phenomenon generated at edges and corners. Numerical examples are supplied. Section 3 describes the procedure for finding particular solutions for the nonhomogeneous Helmholtz equation. It also contains numerical examples, an outline of the complete algorithm, and details of the operation count. In section 4 a mixed Neumann–Dirichlet problem is discussed and solved for the homogeneous Helmholtz equation.

**2. Homogeneous Helmholtz equation.**

**2.1. Mathematical preliminaries.** Let  $\mathcal{C}$  be an open cube

$$(0, \pi) \times (0, \pi) \times (0, \pi) = \{(x, y, z) : 0 \leq x < \pi, 0 < y < \pi, 0 < z < \pi\}$$

(Figure 2.1). We will solve the homogeneous Helmholtz equation in  $\mathcal{C}$

$$(2.1) \quad \Delta \Psi - \lambda^2 \Psi \equiv \Psi''_{xx} + \Psi''_{yy} + \Psi''_{zz} - \lambda^2 \Psi = 0,$$

which is said to be the monotone Helmholtz (MH) equation, and solve

$$(2.2) \quad \Delta \Psi + k^2 \Psi = 0,$$

which is said to be the oscillatory Helmholtz (OH) equation.

Either Dirichlet,

$$(2.3) \quad \begin{aligned} \Psi(0+, y, z) = f_6(y, z), & \quad \Psi(\pi-, y, z) = f_5(y, z), & \quad \Psi(x, 0+, z) = f_4(x, z), \\ \Psi(x, \pi-, z) = f_3(x, z), & \quad \Psi(x, y, 0+) = f_2(x, y), & \quad \Psi(x, y, \pi-) = f_1(x, y), \end{aligned}$$

or Neumann,

$$(2.4) \quad \begin{aligned} \frac{\partial \Psi}{\partial x}(0+, y, z) = f_6(y, z), & \quad \frac{\partial \Psi}{\partial x}(\pi-, y, z) = f_5(y, z), & \quad \frac{\partial \Psi}{\partial x}(x, 0+, z) = f_4(x, z), \\ \frac{\partial \Psi}{\partial x}(x, \pi-, z) = f_3(x, z), & \quad \frac{\partial \Psi}{\partial x}(x, y, 0+) = f_2(x, y), & \quad \frac{\partial \Psi}{\partial x}(x, y, \pi-) = f_1(x, y), \end{aligned}$$

boundary conditions are imposed. Mixed Dirichlet–Neumann boundary conditions can be treated by a similar approach where each face can be associated with one of the two types of boundary conditions. First we will introduce the algorithm for the Dirichlet problem, and later we will describe the changes necessary to accommodate the Neumann or mixed problem.

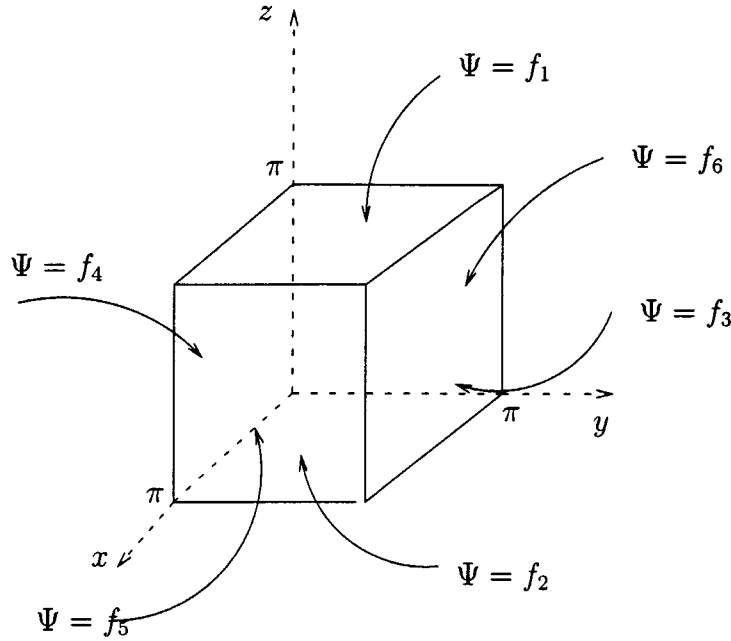


FIG. 2.1. Dirichlet's problem for cube  $C$ . The continuous function  $f$  on  $\partial C$  can be specified by six functions  $f_1, \dots, f_6$ , one on each of the six faces of  $\partial C$ .

We begin by solving a simple canonical problem for (2.1) or (2.2)

$$(2.5) \quad \begin{aligned} \Psi(0+, y, z) = \Psi(\pi-, y, z) = 0, \quad \Psi(x, 0+, z) = \Psi(x, \pi-, z) = 0, \\ \Psi(x, y, 0+) = 0, \quad \Psi(x, y, \pi-) = f_1(x, y). \end{aligned}$$

Evidently the function  $\sin mx \sin ny \sinh \delta_{mn} z$  satisfies (2.1) if

$$\delta_{mn} = \sqrt{n^2 + m^2 + \lambda^2}.$$

The same function with  $\delta_{mn} = \sqrt{n^2 + m^2 - k^2}$  is a solution of the OH equation (2.2) if  $n^2 + m^2 > k^2$ .

In the case  $n^2 + m^2 < k^2$  the function  $\sin mx \sin ny \sin(\sqrt{k^2 - n^2 - m^2} z)$  is a solution.

Any finite superposition of these solutions

$$(2.6) \quad \sum_{m,n=1}^{M,N} D_{mn} \sin mx \sin ny \frac{\sinh \delta_{mn} z}{\sinh \delta_{mn}}$$

is also a solution of the MH equation, and the sum

$$(2.7) \quad \begin{aligned} \sum_{m^2+n^2 < k^2} D_{mn} \sin mx \sin ny \frac{\sin(\sqrt{k^2 - n^2 - m^2} z)}{\sin(\sqrt{k^2 - n^2 - m^2})} \\ + \sum_{m^2+n^2 > k^2} D_{mn} \sin mx \sin ny \frac{\sin(\sqrt{n^2 + m^2 - k^2} z)}{\sin(\sqrt{n^2 + m^2 - k^2})} \end{aligned}$$

is a solution of the OH equation. If  $k$  is a positive integer such that for certain  $n_0, m_0$  the equality  $n_0^2 + m_0^2 = k^2$  holds, then the term  $D_{mn} \sin m_0x \sin n_0y$  can be added to the above solution.

If  $M, N \rightarrow \infty$ , we obtain

$$(2.8) \quad \Psi(x, y, z) = \sum_{m,n=1}^{\infty} D_{mn} \sin mx \sin ny \frac{\sinh \delta_{mn}z}{\sinh \delta_{mn}}$$

as a possible solution of the MH equation and, correspondingly, we obtain (2.7) for the OH equation. Here the coefficients  $D_{mn}$  have to be determined so that for  $z = \pi$  the boundary condition

$$f_1(x, y) = \sum_{m,n=1}^{\infty} D_{mn} \sin mx \sin ny$$

is satisfied. Thus

$$D_{mn} = \frac{4}{\pi^2} \int_0^\pi \int_0^\pi \sin mx \sin ny dx dy.$$

By adding such expressions, we obtain the solution  $\Psi$  for the Dirichlet problem as a sum of six series of the form (2.8) for the MH equation or (2.7) for the OH equation. For instance, the problem (2.1) with

$$\begin{aligned} \Psi(0+, y, z) &= \Psi(\pi-, y, z) = 0, \\ \Psi(x, 0+, z) &= f_4(x, z), \quad \Psi(x, \pi-, z) = 0, \\ \Psi(x, y, 0+) &= \Psi(x, y, \pi-) = 0 \end{aligned}$$

has the series solution

$$\Psi(x, y, z) = \sum_{m,n=1}^{\infty} D_{mn} \sin mx \sin nz \frac{\sinh \delta_{mn}(\pi - y)}{\sinh \delta_{mn}\pi},$$

with

$$D_{mn} = \frac{4}{\pi^2} \int_0^\pi \int_0^\pi f_4(u, v) \sin mu \sin nv du dv.$$

When the solution does not vanish on the other faces we may need more series of this type. The other series solutions that we need are obtained by permuting the variables  $x, y$ , and  $z$  in the two series above.

A sum of six series like the one in (2.7) and (2.8) is a solution of the Helmholtz equation with a given, “general,” boundary function on the surface  $\partial\mathcal{C}$ . The series convergence rate depends on the behavior of the “face functions,”  $f(i)$ . If  $\Psi \equiv 0$  on the edges of the cube together with several normal derivatives of even order, the convergence rate will be very good.

In the next section we describe the procedure for achieving this situation.

**2.2. Subtraction procedure for edges.** Suppose  $\Psi(x, 0, \pi) = \phi_1(x)$ ,  $0 < x < \pi$ . The boundary function can be made to vanish; i.e.,  $\Psi(x, 0, \pi) = 0$ ,  $0 < x < \pi$ , can be achieved by subtraction of one of the following homogeneous solutions:

$$(2.9) \quad u_1(x, y, z) = \sum_{n=1}^{\infty} d_n \sin nx \frac{\sinh \lambda_{1n}(\pi - y)}{\sinh \lambda_{1n}\pi} \frac{\sinh \lambda_{2n}z}{\sinh \lambda_{2n}\pi},$$

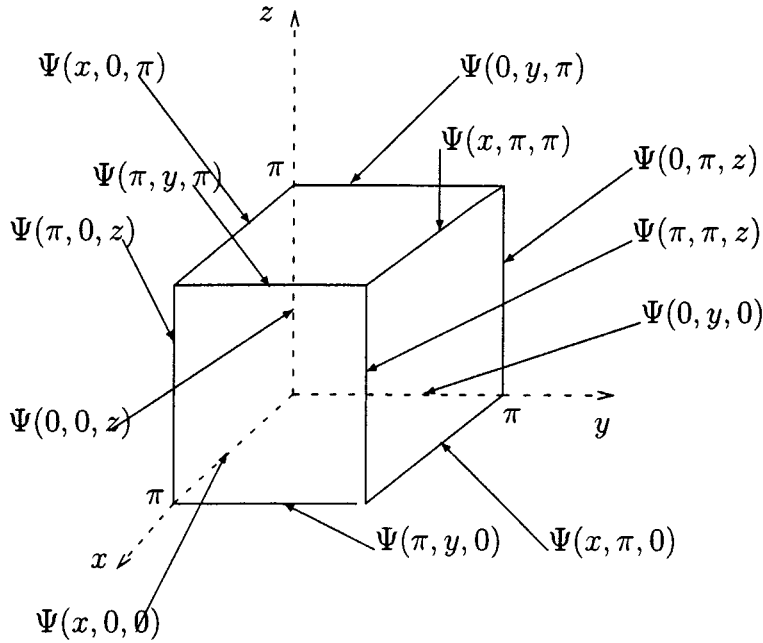


FIG. 2.2. For every edge a function is subtracted from the solution to make the difference satisfy zero boundary conditions on that edge.

where

$$\lambda_{1n}^2 + \lambda_{2n}^2 - n^2 = \begin{cases} \lambda^2 & \text{for MH equation,} \\ -k^2 & \text{for OH equation,} \end{cases}$$

or

$$(2.10) \quad u_1^*(x, y, z) = \sum_{n=1}^{\infty} d_n \sin nx \frac{\sinh \lambda_{1n}(\pi - y)}{\sinh \lambda_{1n}\pi} \frac{\sin \lambda_{2n}z}{\sin \lambda_{2n}\pi}$$

with

$$\lambda_{1n}^2 - \lambda_{2n}^2 - n^2 = \begin{cases} \lambda^2 & \text{for MH equation,} \\ -k^2 & \text{for OH equation.} \end{cases}$$

Here we assumed the nonresonance condition  $\sin \lambda_{2n}\pi \neq 0$ . In the MH case we can use the former series (2.9) with  $\lambda_{1n} = \lambda_{2n} = \sqrt{(\lambda^2 + n^2)/2}$ , while for the OH equation we can use the latter series (2.10) with

$$\begin{aligned} \lambda_{2n} &= 1, & \lambda_{1n} &= \sqrt{n^2 + 1 - k^2}, & n &\geq k, \\ \lambda_{1n} &= 1, & \lambda_{2n} &= \sqrt{1 + k^2 - n^2}, & n &< k. \end{aligned}$$

Here

$$d_n = \frac{2}{\pi} \int_0^\pi \phi_1(x) \sin nx \, dx;$$

$u_1$  and  $u_1^*$  obviously satisfy the corresponding Helmholtz equation and vanish on all the box edges except the chosen one. See Figure 2.2.

Similarly, subtraction functions for the other edges are constructed. For instance, after subtracting

$$(2.11) \quad u_2(x, y, z) = \sum_{n=1}^{\infty} \left[ \frac{2}{\pi} \int_0^{\pi} \phi_1(x) \sin nx dx \right] \sin nx \frac{\sinh \lambda_{1n} y}{\sinh \lambda_{1n} \pi} \frac{\sinh \lambda_{2n} z}{\sinh \lambda_{2n} \pi}$$

the function vanishes on the edge  $(x, \pi, \pi)$ :  $\Psi(x, \pi, \pi) = 0, 0 < x < \pi$ .

After subtracting  $u_1, u_2, \dots, u_{12}$  we obtain the solution that vanishes on the edges (except perhaps in the corners) and coincides with the initial solution on the open faces together with its even derivatives.

Accurate approximation of this solution by series of types (2.9) and (2.10) is possible if both the function values and the even derivatives vanish on the edges. In (2.9)–(2.11)  $\lambda_{1n}$  and  $\lambda_{2n}$  are not defined uniquely. They can be therefore chosen such that the second derivatives achieve the required values. We assume that the boundary function  $f$  satisfies the Helmholtz equation on the edges.

The functions  $\phi_1(x), \frac{\partial^2 \Psi}{\partial y^2}(x, 0, \pi)$  can be presented as

$$(2.12) \quad \phi_1(x) \sim \sum_{n=1}^{\infty} d_n \sin nx, \quad \frac{\partial^2 \Psi}{\partial y^2}(x, 0, \pi) \sim \sum_{n=1}^{\infty} b_n \sin nx,$$

with

$$(2.13) \quad d_n = \frac{2}{\pi} \int_0^{\pi} \phi_1(x) \sin nx dx, \quad b_n = \frac{2}{\pi} \int_0^{\pi} \frac{\partial^2 \Psi}{\partial y^2}(x, 0, \pi) \sin nx dx.$$

For the MH equation we set the following conditions:

In the case  $b_n/d_n > 0$  we choose  $\lambda_{1n}^2 = b_n/d_n$  and

if  $n^2 + \lambda^2 \geq \lambda_{1n}^2$ , then  $\lambda_{2n} = \sqrt{\lambda^2 + n^2 - \lambda_{1n}^2}$ , the solution is (2.9),

if  $n^2 + \lambda^2 < \lambda_{1n}^2$ , then  $\lambda_{2n} = \sqrt{\lambda_{1n}^2 - \lambda^2 - n^2}$ , the solution is (2.10);

in the case  $b_n/d_n < 0$  we choose  $\lambda_{1n}^2 = -b_n/d_n$  and

$$\lambda_{2n} = \sqrt{\lambda_{1n}^2 + \lambda^2 + n^2}, \quad \text{the solution is } \sum_{n=1}^{\infty} d_n \sin nx \frac{\sin \lambda_{1n}(\pi - y)}{\sin \lambda_{1n} \pi} \frac{\sinh \lambda_{2n} z}{\sinh \lambda_{2n} \pi}.$$

For the OH equation we set the following conditions:

In the case  $b_n/d_n > 0$  we choose  $\lambda_{1n}^2 = b_n/d_n$  and

if  $n^2 \geq \lambda_{1n}^2 + k^2$ , then  $\lambda_{2n} = \sqrt{n^2 - \lambda_{1n}^2 - k^2}$ , the solution is (2.9),

if  $n^2 < \lambda_{1n}^2 + k^2$ , then  $\lambda_{2n} = \sqrt{\lambda_{1n}^2 + k^2 - n^2}$ , the solution is (2.10);

in the case  $b_n/d_n < 0$  we choose  $\lambda_{1n}^2 = -b_n/d_n$  and

$$\lambda_{2n} = \sqrt{\lambda_{1n}^2 + k^2 + n^2}, \quad \text{the solution is } \sum_{n=1}^{\infty} d_n \sin nx \frac{\sin \lambda_{1n}(\pi - y)}{\sin \lambda_{1n} \pi} \frac{\sin \lambda_{2n} z}{\sin \lambda_{2n} \pi}.$$

Then, after subtraction of  $u_1$  the boundary function vanishes on the edges together with its second partial derivatives in  $y$  and  $z$ .

The procedure is not applicable if at least one  $d_n = 0$ . In this case the following function can be subtracted for the elimination of the second derivative for the MH equation

$$(2.14) \quad \sum_{n=1}^{\infty} B_n \sin nx \left[ \frac{\sinh \lambda_{1n} y}{\sinh \lambda_{1n} \pi} \frac{\sinh \lambda_{2n}(\pi - z)}{\sinh \lambda_{2n} \pi} - \frac{\sinh \lambda_{3n} y}{\sinh \lambda_{3n} \pi} \frac{\sinh \lambda_{4n}(\pi - z)}{\sinh \lambda_{4n} \pi} \right],$$

with  $\lambda_{1n} \neq \lambda_{3n}, \lambda_{2n}$ , and  $B_n, \lambda_{4n}$  being such that

$$B_n = \frac{b_n}{\lambda_{1n}^2 - \lambda_{3n}^2}, \lambda_{1n}^2 + \lambda_{2n}^2 - \lambda^2 = n^2, \quad \lambda_{3n}^2 + \lambda_{4n}^2 - \lambda^2 = n^2.$$

For the OH equation we subtract

$$(2.15) \quad \sum_{n=1}^{\infty} B_n \sin nx \left[ \frac{\sinh \lambda_{1n} y}{\sinh \lambda_{1n} \pi} \frac{\sin \lambda_{2n}(\pi - z)}{\sin \lambda_{2n} \pi} - \frac{\sin \lambda_{2n} y}{\sin \lambda_{2n} \pi} \frac{\sinh \lambda_{1n}(\pi - z)}{\sinh \lambda_{1n} \pi} \right],$$

with  $B_n = b_n/(\lambda_{1n}^2 + \lambda_{2n}^2)$ , and  $\lambda_{1n}, \lambda_{2n}$  being such that  $\sin \lambda_{2n} \pi \neq 0, \lambda_{1n}^2 - \lambda_{2n}^2 = n^2 - k^2$ .

A boundary function defined on an interval (i.e., along the edge) can be well approximated by a sine series (2.12) if it vanishes in the ends (preferably together with some of its even derivatives). In the next section we describe the procedure for obtaining such a behavior at the end points of the edges, i.e., the corners of the cube.

It is appropriate to comment at this point that in the present paper the functions describing the boundary conditions on the faces are assumed to satisfy compatibility conditions. For example, the functions on two faces intersecting at an edge must be continuous across the edge and, furthermore, the relevant second derivatives must add up with the function values to satisfy the Helmholtz equation on all edges and corners; otherwise a singular behavior can be expected which will prevent fast convergence. Such a behavior will affect all methods of solution. A possible approach which we used in our previous papers is to address first all such singularities by a preliminary analytical subtraction of appropriate singular solutions.

**2.3. Subtraction procedure for the corners.** Suppose  $\Psi(0, 0, 0) = A$ . For the MH equation a zero value at the origin is achieved by subtracting the so-called corner function defined as

$$(2.16) \quad C_{(0,0,0)}(x, y, z) = A \left[ \frac{\sinh \lambda_1(\pi - x)}{\sinh \lambda_1 \pi} \frac{\sinh \lambda_2(\pi - y)}{\sinh \lambda_2 \pi} \frac{\sinh \lambda_3(\pi - z)}{\sinh \lambda_3 \pi} \right]$$

with  $\lambda_1^2 + \lambda_2^2 + \lambda_3^2 = \lambda^2$ . For the OH equation

$$(2.17) \quad C_{(0,0,0)}(x, y, z) = A \left[ \frac{\sinh \lambda_1(\pi - x)}{\sinh \lambda_1 \pi} \frac{\sinh \lambda_2(\pi - y)}{\sinh \lambda_2 \pi} \frac{\sin \lambda_3(\pi - z)}{\sin \lambda_3 \pi} \right]$$

with  $\lambda_1^2 + \lambda_2^2 + k^2 = \lambda_3^2, \sin \lambda_3 \pi \neq 0$ . The subtraction of such a function does not influence the values at the other seven corners; therefore, each corner can be treated separately and independently. See Figure 2.3.

Let  $A \neq 0$ . Then by appropriate choice of  $\lambda_1, \lambda_2$  in (2.17) we achieve the coincidence of the second derivatives. Namely, if  $B_x = \frac{\partial^2 \Psi}{\partial x^2}(0, 0, 0), B_y = \frac{\partial^2 \Psi}{\partial y^2}(0, 0, 0) > 0, B_z = \frac{\partial^2 \Psi}{\partial z^2}(0, 0, 0) > 0$ , then we choose for the MH equation the ‘‘corner function’’ as

$$(2.18) \quad C_{(0,0,0)}(x, y, z) = A \left[ \frac{\mathcal{S}_1(\lambda_1(\pi - x))}{\mathcal{S}_1(\lambda_1 \pi)} \frac{\mathcal{S}_2(\lambda_2(\pi - y))}{\mathcal{S}_2(\lambda_2 \pi)} \frac{\mathcal{S}_3(\lambda_3(\pi - z))}{\mathcal{S}_3(\lambda_3 \pi)} \right],$$



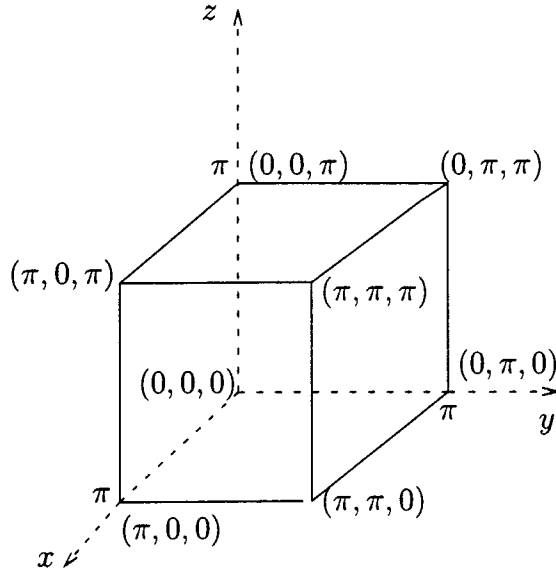


FIG. 2.3. For every corner a function is subtracted from the solution to make the difference satisfy zero boundary conditions at that corner.

where

$$\lambda_1^2 = |B_x/A|, \quad \lambda_2^2 = |B_y/A|, \quad \lambda_3^2 = |B_z/A|, \quad \lambda_1 = \sqrt{\lambda_3^2 + \lambda_2^2 - \lambda^2},$$

and

$$\mathcal{S}_1(x) = \begin{cases} \sinh x, & B_x/A > 0, \\ \sin x, & B_x/A < 0. \end{cases}$$

$\mathcal{S}_2, \mathcal{S}_3$  are introduced similarly.

The same technique can be applied to the OH equation. In the practical implementation the following algorithm was employed.

If  $\Psi(0, 0, 0) = 0$  then the vanishing second derivative is achieved by subtracting a linear combination of the corner functions.

We will begin with the MH equation. Let  $B_x$  stand for  $\frac{\partial^2 \Psi}{\partial x^2}(0, 0, 0)$ , and let  $B_y$  stand for  $\frac{\partial^2 \Psi}{\partial y^2}(0, 0, 0)$ . Then the following function is subtracted:

$$C_{(0,0,0)}(x, y, z) = a \left[ \frac{\sinh \lambda_1(\pi - x)}{\sinh \lambda_1 \pi} \frac{\sinh \lambda_2(\pi - y)}{\sinh \lambda_2 \pi} \frac{\sinh \lambda_3(\pi - z)}{\sinh \lambda_3 \pi} - \frac{\sinh \lambda_2(\pi - x)}{\sinh \lambda_2 \pi} \frac{\sinh \lambda_3(\pi - y)}{\sinh \lambda_3 \pi} \frac{\sinh \lambda_1(\pi - z)}{\sinh \lambda_1 \pi} \right],$$

with

$$\lambda_1^2 = \frac{\lambda^2}{3} + \frac{2B_x + B_y}{3a}, \quad \lambda_2^2 = \frac{\lambda^2}{3} + \frac{B_y - B_x}{3a}, \quad \lambda_3^2 = \frac{\lambda^2}{3} - \frac{B_x + 2B_y}{3a}.$$

This is a solution for the MH equation since

$$\lambda_1^2 + \lambda_2^2 + \lambda_3^2 = \frac{\lambda^2}{3} + \frac{\lambda^2}{3} + \frac{\lambda^2}{3} + \frac{2B_x + B_y + B_y - B_x - B_x - 2B_y}{3a} = \lambda^2.$$

Constant  $a$  is chosen such that  $\lambda_i^2 > 0$ ,  $i = 1, 2, 3$ . For example, if  $a = 3(|B_x| + |B_y|)/\lambda^2$ , then

$$\lambda_1^2 = \frac{\lambda^2}{3} \left( 1 + \frac{2B_x + B_y}{3(|B_x| + |B_y|)} \right) > 0,$$

$$\lambda_2^2 = \frac{\lambda^2}{3} \left( 1 + \frac{B_y - B_x}{3(|B_x| + |B_y|)} \right) > 0,$$

$$\lambda_3^2 = \frac{\lambda^2}{3} \left( 1 - \frac{B_x + 2B_y}{3(|B_x| + |B_y|)} \right) > 0.$$

Consider the OH equation. We will consider four cases according to the signs of  $(B_y - B_x)$  and  $(2B_x + B_y)$ .

*Case 1.* Let  $(B_y - B_x)(2B_x + B_y) > 0$ . We subtract the following function

$$a \left[ \frac{\sinh \lambda_1(\pi - x)}{\sinh \lambda_1 \pi} \frac{\sinh \lambda_2(\pi - y)}{\sinh \lambda_2 \pi} \frac{\sin \lambda_3(\pi - z)}{\sin \lambda_3 \pi} - \frac{\sinh \lambda_2(\pi - x)}{\sinh \lambda_2 \pi} \frac{\sin \lambda_3(\pi - y)}{\sin \lambda_3 \pi} \frac{\sinh \lambda_1(\pi - z)}{\sinh \lambda_1 \pi} \right],$$

with  $a$  being of the same sign as  $(B_y - B_x)$ ,

$$\lambda_1^2 = \frac{2B_x + B_y}{3a} - \frac{k^2}{3}, \quad \lambda_2^2 = \frac{B_y - B_x}{3a} - \frac{k^2}{3}, \quad \lambda_3^2 = \frac{k^2}{3} + \frac{B_x + 2B_y}{3a}.$$

The constant  $a$  again is chosen as

$$a = \frac{\min\{|B_y - B_x|, |2B_x + B_y|\} \operatorname{sgn}(B_y - B_x)}{2k^2};$$

therefore,  $\lambda_i$  are positive since

$$\frac{2B_x + B_y}{3a} \geq \frac{2k^2}{3}, \quad \frac{B_y - B_x}{3a} \geq \frac{2k^2}{3}, \quad \frac{B_x + 2B_y}{3a} > 0.$$

*Case 2.* Let  $(B_y - B_x)(2B_x + B_y) < 0$ . We choose  $a$  of the same sign as  $B_x - B_y$  such that

$$\lambda_1^2 = \frac{2B_x + B_y}{3a} - \frac{k^2}{3} > 0, \quad \lambda_2^2 = \frac{B_x - B_y}{3a} + \frac{k^2}{3} > 0, \quad \frac{k^2}{3} + \frac{B_x + 2B_y}{3a} \neq 0$$

(in fact any  $a$  such that  $|a| < |2B_x + B_y|/k^2$ ,  $|a| < |B_x - B_y|/k^2$ ,  $|a| \neq (B_x + 2B_y)/k^2$  will do).

If  $(B_x + 2B_y)/3a + k^2/3 > 0$ , then we choose

$$\lambda_3^2 = \frac{k^2}{3} + \frac{B_x + 2B_y}{3a}$$

and subtract

$$a \left[ \frac{\sinh \lambda_1(\pi - x)}{\sinh \lambda_1 \pi} \frac{\sin \lambda_2(\pi - y)}{\sin \lambda_2 \pi} \frac{\sin \lambda_3(\pi - z)}{\sin \lambda_3 \pi} - \frac{\sin \lambda_2(\pi - x)}{\sin \lambda_2 \pi} \frac{\sin \lambda_3(\pi - y)}{\sin \lambda_3 \pi} \frac{\sinh \lambda_1(\pi - z)}{\sinh \lambda_1 \pi} \right],$$

else we choose

$$\lambda_3^2 = -\frac{k^2}{3} - \frac{B_x + 2B_y}{3a}$$

and subtract the following function

$$a \left[ \frac{\sinh \lambda_1(\pi - x)}{\sinh \lambda_1 \pi} \frac{\sin \lambda_2(\pi - y)}{\sin \lambda_2 \pi} \frac{\sinh \lambda_3(\pi - z)}{\sinh \lambda_3 \pi} - \frac{\sin \lambda_2(\pi - x)}{\sin \lambda_2 \pi} \frac{\sinh \lambda_3(\pi - y)}{\sinh \lambda_3 \pi} \frac{\sinh \lambda_1(\pi - z)}{\sinh \lambda_1 \pi} \right].$$

*Case 3.* Suppose  $B_y = B_x$ .

Then we can, in particular, choose

$$C_{(0,0,0)}(x, y, z) = \frac{B_x}{2 + k^2/2} \left[ \frac{\sinh(\pi - x)}{\sinh \pi} \frac{\sinh(\pi - y)}{\sinh \pi} \frac{\sin(\sqrt{2 + k^2}(\pi - z))}{\sin(\sqrt{1 + k^2/2}\pi)} - \frac{\sin \sqrt{1 + k^2/2}(\pi - x)}{\sin \sqrt{1 + k^2/2}\pi} \frac{\sin \sqrt{1 + k^2/2}(\pi - y)}{\sin \sqrt{1 + k^2/2}\pi} \frac{\sinh(\sqrt{2}(\pi - z))}{\sinh(\sqrt{2}\pi)} \right].$$

*Case 4.* Suppose  $2B_x + B_y = 0$ .

We choose  $\lambda > k$ ,  $a = B_x/(2\lambda^2)$  and subtract

$$C_{(0,0,0)}(x, y, z) = a \left[ \frac{\sinh \lambda(\pi - x)}{\sinh \lambda \pi} \frac{\sin \sqrt{2}\lambda(\pi - y)}{\sin \sqrt{2}\lambda \pi} \frac{\sinh(\sqrt{\lambda^2 - k^2}(\pi - z))}{\sinh(\sqrt{\lambda^2 - k^2}\pi)} - \frac{\sin \lambda(\pi - x)}{\sin \lambda \pi} \frac{\sinh \lambda(\pi - y)}{\sinh \lambda \pi} \frac{\sin(\sqrt{\lambda^2 - k^2}(\pi - z))}{\sin(\sqrt{\lambda^2 - k^2}\pi)} \right].$$

We recall that  $\lambda \neq n$  and everywhere above the nonresonance condition for the sine is satisfied.

The same functions are subtracted from the other corners, where  $x$  is replaced by  $\pi - x$ ,  $y$  by  $\pi - y$ , and  $z$  by  $\pi - z$ .

For computing derivatives the method of divided differences was found to be sufficiently accurate when coupled with the subtraction approach. The five-point stencil was used for the second derivative. More accurate derivatives can be computed in principle by using global spectral methods. These methods can achieve a spectral convergence rate as  $N$  is increased, but only if the Gibbs phenomenon can be controlled.

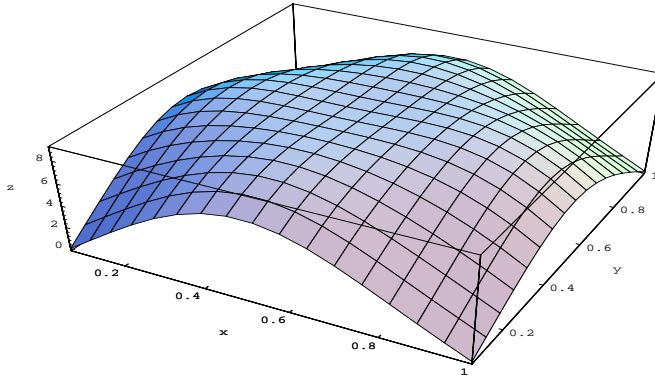


FIG. 2.4. The function values on the  $z = 0$  face after subtraction of corner functions.

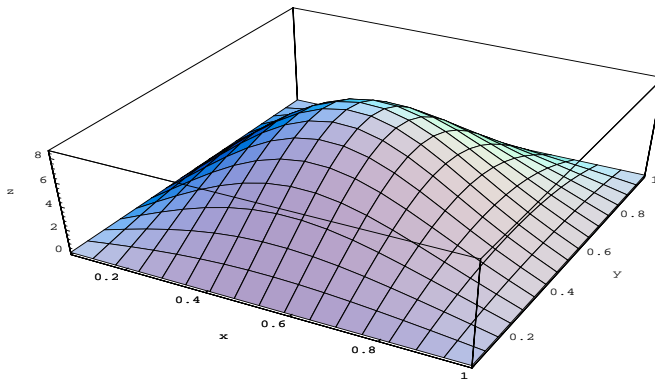


FIG. 2.5. The values on the  $z = 0$  face after subtraction of edge functions.

An algorithm which resolves the Gibbs phenomenon was developed in [8, 9]. The basic concept of this approach consists of reexpansion of the Fourier partial sums into the rapidly convergent Gegenbauer series. In [14] this algorithm was extended to the evaluation of the spatial derivatives of piecewise analytic functions. The application of this method makes it possible to achieve the spectral accuracy when computing the second (the fourth, etc.) derivative.

Figures 2.4 and 2.5 illustrate the absolute value of the boundary function on the face  $z = 0$  after subtraction of the corner functions and the edge functions, respectively, for the numerical solution of (1.1) with  $\lambda = 1$  in the cube  $[0, 1] \times [0, 1] \times [0, 1]$  which corresponds to the exact solution

$$\cos(\lambda_1 x) \cos(\lambda_2 y) \frac{\sinh(\lambda_3(1-z))}{\sinh(\lambda_3)}, \quad \lambda_1 = 2\pi, \quad \lambda_2 = \sqrt{5\pi^2 - 1}, \quad \lambda_3 = 3\pi.$$

**2.4. Numerical results.** It was shown in [4] that the error in the results obtained by our numerical algorithm is due mainly to the truncation of the Fourier series used to represent the solution. The convergence rate of the approximate solution to

TABLE 2.1

Numerical accuracy for the exact solution (2.20) of the MH equation (2.19).

$N_x \times N_y \times N_z$	One subtr. step			Two subtr. steps		
	$\varepsilon_{MAX}$	$\varepsilon_{MSQ}$	$\varepsilon_{L^2}$	$\varepsilon_{MAX}$	$\varepsilon_{MSQ}$	$\varepsilon_{L^2}$
$8 \times 8 \times 8$	1.0e-4	1.2e-5	1.4e-6	6e-7	5.5e-8	6.8e-9
$16 \times 16 \times 16$	3.0e-5	1.6e-6	2.1e-7	4.2e-8	1.9.0e-9	2.4e-10
$32 \times 32 \times 32$	7.8e-6	2.1e-7	2.8e-8	2.7e-9	6.3e-11	8.3e-12
$64 \times 64 \times 64$	2.0e-6	2.7e-8	3.6e-9	1.7e-10	3.4e-12	4.6e-13

TABLE 2.2

Numerical accuracy for the exact solution (2.21) of the MH equation (2.19).

$N_x \times N_y \times N_z$	$\varepsilon_{MAX}$	$\varepsilon_{MSQ}$	$\varepsilon_{L^2}$
$8 \times 8 \times 8$	4.2e-5	4.3e-6	3.3e-5
$16 \times 16 \times 16$	3.5e-6	1.3e-7	1.2e-6
$32 \times 32 \times 32$	2.5e-7	4.3e-9	4.6e-8
$64 \times 64 \times 64$	1.7e-8	1.4e-10	1.5e-9
$128 \times 128 \times 128$	1.0e-9	3.3e-11	3.8e-10

the Helmholtz equation was found to be the same as in the particular case of the Laplace equation which was evaluated in [4] using the theory and estimates in [7]. According to these estimates, the results obtained when the number of points in each direction is doubled are four times more accurate when one subtraction step is used and 16 times more accurate when two subtraction steps are used.

Assume that  $\Psi$  is the exact solution and  $\Psi'$  is the computed one. In the numerical examples we will use the following measures to estimate the errors:

$$\begin{aligned} \varepsilon_{MAX} &= \max \|\Psi'_i - \Psi_i\|, \\ \varepsilon_{MSQ} &= \sqrt{\frac{\sum_{i=1}^N (\Psi'_i - \Psi_i)^2}{n}}, \\ \varepsilon_{L^2} &= \sqrt{\frac{\sum_{i=1}^N (\Psi'_i - \Psi_i)^2}{\sum_{i=1}^N \Psi_i^2}}. \end{aligned}$$

**2.4.1. Monotone Helmholtz equation.**

*Example 1.* Consider the solution of the MH equation

$$(2.19) \quad \Delta u - \lambda^2 u = 0, \quad \lambda = 2,$$

with boundary conditions corresponding to the exact solution

$$(2.20) \quad u(x, y, z) = \exp \left( \lambda \left( \sqrt{\frac{1}{2}}x + \sqrt{\frac{1}{3}}y + \sqrt{\frac{1}{6}}z \right) \right).$$

The numerical results are given in Table 2.1.

*Example 2.* We solve the MH equation with  $\lambda = 1$  and the boundary conditions corresponding to the exact solution

$$(2.21) \quad u(x, y, z) = \cos 2x \frac{\sinh \sqrt{\lambda^2 + 3}y \sinh z}{\sinh \sqrt{\lambda^2 + 3}\pi \sinh \pi}.$$

We use a two subtraction step algorithm. The results are given in Table 2.2.

TABLE 2.3

Dependence on  $\lambda$  of the accuracy for the MH equation with the exact solution (2.21).

$N_x \times N_y \times N_z$	$\lambda^2$	$\varepsilon_{MAX}$	$\varepsilon_{MSQ}$	$\varepsilon_{\mathcal{L}^2}$
$32 \times 32 \times 32$	4	2.6e-7	4.6e-9	5e-8
	16	3.5e-7	6.2e-9	7e-8
	64	8.6e-7	1.7e-8	2e-7
	100	1.4e-6	3.0e-8	4e-7
	256	5.6e-6	1.3e-7	2e-6
$64 \times 64 \times 64$	4	1.8e-8	1.5e-10	1.7e-9
	16	2.3e-8	2.0e-10	2.4e-9
	64	5.8e-8	5.3e-10	7.6e-9
	100	9.7e-8	9.0e-10	1.4e-8
	256	4.0e-7	4.0e-9	7.4e-8

TABLE 2.4

Numerical accuracy for the trigonometrical exact solution (2.23) of the OH equation (2.22).

$N_x \times N_y \times N_z$	One subtr. step			Two subtr. steps		
	$\varepsilon_{MAX}$	$\varepsilon_{MSQ}$	$\varepsilon_{\mathcal{L}^2}$	$\varepsilon_{MAX}$	$\varepsilon_{MSQ}$	$\varepsilon_{\mathcal{L}^2}$
$8 \times 8 \times 8$	2.8e-4	3.9e-5	1.9e-6	7.1e-5	1.0e-5	5.0e-5
$16 \times 16 \times 16$	9.5e-5	6.5e-6	3.8e-5	5.1e-6	3.2e-7	1.9e-6
$32 \times 32 \times 32$	2.8e-5	9.0e-7	5.9e-6	3.4e-7	1.1e-8	7.2e-8
$64 \times 64 \times 64$	7.2e-6	1.2e-7	8.0e-7	2.2e-8	3.6e-10	2.5e-9

Table 2.3 shows the dependence on  $\lambda$  of the accuracy when the exact solution of the MH equation is given by (2.21).

From the above numerical results we can see that a good accuracy ( $10^{-7}$ ) is achieved with a small number of grid points (16–32 in each direction) especially for nonhighly oscillating solutions. The error does not depend strongly on the size of  $\lambda$ , so high accuracy is also preserved for large  $\lambda$ . For the maximal error the convergence rate is slightly worse than the predicted rate, but it is about two times better than predicted for the “average” errors  $\varepsilon_{MSQ}$  and  $\varepsilon_{\mathcal{L}^2}$ .

#### 2.4.2. Oscillatory Helmholtz equation.

*Example 3.* Consider the solution of the OH equation

$$(2.22) \quad \Delta u + k^2 u = 0, \quad k = 1,$$

with the boundary conditions corresponding to the exact solution

$$(2.23) \quad u(x, y, z) = \cos(2x) \cos\left(\sqrt{1+k^2} y\right) \frac{\sinh \sqrt{5}z}{\sinh \sqrt{5}\pi}.$$

The numerical accuracy for the OH equation (2.22) with the exact solution (2.23) is shown in Table 2.4.

Table 2.5 shows the dependency of the accuracy on  $k$ .

*Example 4.* We solve the OH equation with  $k = 2$  and boundary conditions corresponding to the exact solution

$$(2.24) \quad u(x, y, z) = \exp(0.8x + 0.6y) \sin\left(\sqrt{1+k^2}z\right).$$

We use the algorithm with two subtraction steps. The results are given in Table 2.6.

The numerical results for the OH equation show the same convergence behavior as in the case of the MH equation. As could be expected, the results for the oscillatory equation are slightly less accurate. However, for an accuracy of  $10^{-7}$  a grid of 32 points in each direction is sufficient.

TABLE 2.5

Dependence of the accuracy on  $k$  for the OH (2.22) with the exact solution (2.23).

$N_x \times N_y \times N_z$	$k^2$	$\varepsilon_{MAX}$	$\varepsilon_{MSQ}$	$\varepsilon_{L^2}$
$32 \times 32 \times 32$	4	3.6e-7	1.3e-8	8e-8
	16	1.0e-6	5.2e-8	3.6e-7
	64	2.2e-6	8.7e-8	6.0e-7
	100	2.0e-6	8.0e-8	5.0e-7
	256	1.0e-5	1.4e-6	9.0e-6
$64 \times 64 \times 64$	4	2.2e-8	4.2e-10	2.8e-9
	16	6.5e-8	1.4e-9	9.9e-9
	64	1.2e-7	1.9e-9	1.4e-8
	100	1.6e-7	2.0e-9	1.4e-8
	256	4.6e-7	2.4e-8	1.7e-7

TABLE 2.6

Numerical accuracy for the exact solution (2.24) of the OH (2.22).

$N_x \times N_y \times N_z$	$\varepsilon_{MAX}$	$\varepsilon_{MSQ}$	$\varepsilon_{L^2}$
$8 \times 8 \times 8$	1.1e-6	1.6e-7	9.6e-8
$16 \times 16 \times 16$	8.3e-8	5.0e-9	2.9e-9
$32 \times 32 \times 32$	5.6e-9	1.6e-10	9.5e-11
$64 \times 64 \times 64$	3.6e-10	5.4e-12	3.2e-12

### 3. Nonhomogeneous Helmholtz equations.

**3.1. A Fourier method for the Helmholtz equation in a cube.** As was mentioned above, the Fourier method for the solution of the Helmholtz equation has the advantage that the corresponding operator has a diagonal matrix representation in the Fourier basis. We seek a solution for the nonhomogeneous Helmholtz equation

$$(3.1) \quad \Delta u - \lambda^2 u = F(x, y, z)$$

or for the oscillatory Helmholtz equation

$$(3.2) \quad \Delta u + k^2 u = F(x, y, z).$$

Suppose that both the solutions and the right-hand sides are decomposed into sine series

$$u(x, y, z) = \sum_{l,m,n=1}^{\infty} d_{lmn} \sin(kx) \sin(my) \sin(nz),$$

$$F(x, y, z) = \sum_{l,m,n=1}^{\infty} D_{lmn} \sin(kx) \sin(my) \sin(nz),$$

which are substituted into the Helmholtz equations (3.1) and (3.2). Assume that  $u$  is twice continuously differentiable. Then for (3.1) we have

$$d_{lmn} = \frac{D_{lmn}}{l^2 + m^2 + n^2 - \lambda^2}$$

and for (3.2) we have

$$d_{lmn} = \frac{D_{lmn}}{l^2 + m^2 + n^2 + k^2}.$$

Thus,

$$(3.3) \quad u(x, y, z) = \sum_{l,m,n=1}^{\infty} \frac{D_{lmn}}{l^2 + m^2 + n^2 + \lambda^2} \sin(lx) \sin(my) \sin(nz)$$

or

$$(3.4) \quad u(x, y, z) = \sum_{l,m,n=1}^{\infty} \frac{D_{kmn}}{k^2 + m^2 + n^2 - k^2} \sin(lx) \sin(my) \sin(nz).$$

Approximation of the particular solution by the truncated series is accurate if  $F$  vanishes, together with some of its even derivatives, on the faces of the cube which cannot be guaranteed for an arbitrary right-hand side. The approach we use to avoid the Gibbs phenomenon is the following: First we extend the right-hand side to an extended cube  $[-\varepsilon, \pi + \varepsilon] \times [-\varepsilon, \pi + \varepsilon] \times [-\varepsilon, \pi + \varepsilon]$  such that the extended function vanishes together with some of its even derivatives on the new boundary. Then the solution is found in the extended domain by the truncated sine series. Its restriction to the original domain is a particular solution of the nonhomogeneous Helmholtz equation.

The process of constructing a function which coincides with a given function in the original domain and vanishes together with some derivatives on the boundary of the extended domain is described in the Appendix for the 1D case. The details of how to adapt this algorithm to a 3D case are described in the algorithm outline (section 3.2).

### 3.2. The steps of the algorithm and an operation count.

1.  $F(x, y, z)$  is continuously extended to the domain  $[-2\varepsilon, \pi + 2\varepsilon] \times [-2\varepsilon, \pi + 2\varepsilon] \times [-2\varepsilon, \pi + 2\varepsilon]$ . This step can be omitted if the right-hand side is defined in the extended domain.
2. A 1D folding procedure in the  $z$  direction is applied to the extended function  $\bar{F}(x, y, z)$  for each  $-2\varepsilon \leq x, y \leq \pi + 2\varepsilon$ . It is described in the Appendix. As a result, a new function  $\bar{F}_1(x, y, z)$  is obtained which coincides with the original function on the cube  $[0, \pi] \times [0, \pi] \times [0, \pi]$  and  $\bar{F}_1^{(2r)}(x, y, -\varepsilon) = \bar{F}_1^{(2r)}(x, y, \pi + \varepsilon) = 0$ ,  $r = 0, 1, \dots$ ,  $-2\varepsilon \leq x, y \leq \pi + 2\varepsilon$ . The cost of this step is  $O((N + N_\varepsilon)^2 \cdot N_\varepsilon)$ , where  $N_\varepsilon$  is the number of discretization points on the extended segment.  $N_\varepsilon$  is small in comparison with  $N$  (see equation (A.1) in the Appendix).
3. The same folding procedure is applied in the  $y$  direction. For each  $-2\varepsilon \leq x \leq \pi + 2\varepsilon$ ,  $-\varepsilon \leq z \leq \pi + \varepsilon$ , we get the function  $\bar{F}_2$  which is periodic together with its even derivatives in  $y$ :  $\bar{F}_2^{(2r)}(x, -\varepsilon, z) = \bar{F}_2^{(2r)}(x, \pi + \varepsilon, z) = 0$ ,  $r = 0, 1, \dots$ ,  $-2\varepsilon \leq x \leq \pi + 2\varepsilon$ ,  $-\varepsilon \leq z \leq \pi + \varepsilon$ . The cost is  $O((N + N_\varepsilon) \cdot N \cdot N_\varepsilon)$ .
4. Application of the folding procedure in the  $x$  direction requires that for each  $-\varepsilon \leq y, z \leq \pi + \varepsilon$  we get the function  $\bar{F}_3$  periodic in “the extended cube”

$$[-\varepsilon, \pi + \varepsilon] \times [-\varepsilon, \pi + \varepsilon] \times [-\varepsilon, \pi + \varepsilon]$$

together with its even derivatives in the  $x, y$ , and  $z$  directions. The cost of this step is  $O(N^2 \cdot N_\varepsilon)$ .

5. The nonhomogeneous Helmholtz equation (3.1) is solved in the extended domain; the solution is effective and accurate due to the periodicity of the



extended right-hand side  $\bar{F}_3$  which coincides with the original right-hand side in the original domain. The restriction of the solution found to the cube  $[0, \pi] \times [0, \pi] \times [0, \pi]$  is a particular solution of the inhomogeneous Helmholtz equation which does not satisfy boundary conditions. This procedure requires  $O(N^3 \log_2 N)$  operations.

6. Boundary conditions for the homogeneous Helmholtz equation are computed as the difference between the original conditions and those that were generated by the particular solution of the Poisson equation found in the previous step. Corner functions, which are defined by (2.15), are constructed as part of the solution. This step requires  $8 \cdot O(N^3) + O(N^2)$  operations.
7. The second derivatives in two directions are computed for each corner using the divided differences method and it is performed by  $8 \cdot O(N^3)$  operations.
8. Second derivatives at the corners vanish after subtracting functions defined in section 2.3. This requires  $8 \cdot O(N^3)$  operations.
9. The discrete sine transform (DST) is applied on each of the 12 edges, and the subtraction of the “edge functions” (2.9) or (2.10) requires  $12 \cdot O(N^3 \log_2 N)$  operations.
10. Second derivatives in the normal direction are computed for the 12 edges. This requires  $12 \cdot O(N)$  operations.
11. Twelve functions defined by (2.14) are subtracted. This requires  $12 \cdot O(N^3 \log_2 N)$  operations.
12. The 2D DST on the six faces is applied to the remaining boundary function; this requires  $6 \cdot O(N^3 \log_2 N)$  operations.

Therefore, the total computational cost of the algorithm is  $32 \cdot O(N^3 \log_2 N) + O(N^3)$ , i.e.,  $O(N^3 \log_2 N)$  operations.

### 3.3. Numerical results for the nonhomogeneous equation.

#### 3.3.1. Monotone Helmholtz.

*Example 5.* The right-hand side corresponds to the exact solution

$$(3.5) \quad \Psi(x, y, z) = \exp \left\{ -\alpha \left( (x - 0.5)^2 + (y - 0.5)^2 + (z - 0.5)^2 \right) \right\},$$

where  $\lambda = 1.0$ . The results are obtained by application of the algorithm for computing the particular solution of a nonhomogeneous equation followed by the algorithm for the Laplace equation.

Table 3.1 exhibits the dependence of the numerical accuracy on the number of grid points and the steepness of the Gaussian in (3.5).

For  $\alpha = 3$  Table 3.2 describes the dependency between the accuracy and the length of the extended interval  $N_\epsilon$ , where (3.5) is solved. Everywhere below we take  $(32 + 1)^3$  points in the box  $[0, 1]^3$ , while the number of folding points (equal in each direction) varies.

For  $\alpha = 15$  Table 3.3 describes the dependence of the accuracy and the distance of  $(x_0, y_0, z_0)$  to the boundaries (we take the extreme case: the point approaches a corner). Everywhere below  $(16 + 1)^3$  points are taken in the box  $[0, 1]^3$  and we use eight folding points.

*Example 6.* Consider a right-hand side corresponding to the exact solution for  $\lambda = 1$  which is a sum of 12 random Gaussians:

$$(3.6) \quad \Psi(x, y, z) = \sum_{i=1}^{12} \exp \left\{ -\alpha_i \left( (x - x_i)^2 + (y - y_i)^2 + (z - z_i)^2 \right) \right\}.$$

TABLE 3.1

Dependence of the numerical accuracy on the number of grid points and the steepness of the Gaussian in (3.5).

$\alpha$	$N_x \times N_y \times N_z$	Number of fold. points	$\varepsilon_{MAX}$	$\varepsilon_{MSQ}$	$\varepsilon_{L^2}$
0.5	$8 \times 8 \times 8$	4	5.7e-6	2.4e-6	2.8e-6
	$16 \times 16 \times 16$	8	2.1e-8	3.4e-9	3.9e-9
	$32 \times 32 \times 32$	16	9.9e-10	5.1e-11	5.8e-11
3	$8 \times 8 \times 8$	4	3.2e-6	1.4e-6	2.9e-6
	$16 \times 16 \times 16$	8	4.0e-9	1.5e-9	3.0e-9
	$32 \times 32 \times 32$	16	1.1e-10	4.3e-12	8.2e-12
15	$8 \times 8 \times 8$	4	2.8e-6	4.1e-7	2.7e-6
	$16 \times 16 \times 16$	8	1.6e-12	4.8e-13	2.8e-12
	$32 \times 32 \times 32$	16	6.0e-15	4.9e-16	2.8e-15
50	$8 \times 8 \times 8$	4	2.5e-2	1.2e-3	1.9e-2
	$16 \times 16 \times 16$	8	2.6e-7	1.6e-8	2.3e-7
	$32 \times 32 \times 32$	16	7.8e-16	3.0e-16	4.2e-15

TABLE 3.2

Dependence of the numerical accuracy on the number of folding points for  $\alpha = 3$ .

Number of fold. points	$\varepsilon_{MAX}$	$\varepsilon_{MSQ}$	$\varepsilon_{L^2}$
4	2.4e-7	6.8e-8	1.3e-7
8	3.0e-9	2.2e-10	4.2e-10
11	7.7e-10	3.4e-11	6.4e-11
14	2.5e-10	1.0e-11	2.0e-11
16	1.1e-10	4.3e-12	8.2e-12
20	1.9e-11	6.4e-13	1.2e-12

TABLE 3.3

Dependence of the numerical accuracy on the distance of the centers of the Gaussian bells to the boundary for  $\alpha = 15$ .

$(x_0, y_0, z_0)$	$\varepsilon_{MAX}$	$\varepsilon_{MSQ}$	$\varepsilon_{L^2}$
(0.5,0.5,0.5)	1.6e-12	4.8e-13	2.8e-12
(0.4,0.4,0.4)	2.9e-12	5.9e-13	3.5e-12
(0.3,0.3,0.3)	1.5e-10	2.2e-11	1.3e-10
(0.2,0.2,0.2)	1.8e-9	1.8e-10	1.2e-9
(0.1,0.1,0.1)	6.8e-9	4.2e-10	3.2e-9
(0.05,0.05,0.05)	5.9e-9	3.1e-10	2.9e-9
(0.01,0.01,0.01)	2.2e-9	1.4e-10	1.6e-9
(0.001,0.001,0.001)	2.9e-9	1.6e-10	2.0e-9
(0.0001,0.0001,0.0001)	3.0e-9	1.6e-10	2.1e-9
(1.e-5,1.e-5,1.e-5)	3.0e-9	1.6e-10	2.1e-9

In the numerical example below,

$$\alpha = 2.0, 16.0, 0.04, 4.5, 9.7, 26.3, 2.9, 1.2, 17.5, 6.2, 29.7, 19.6,$$

and the centers of the Gaussians

$$(0.23,0.54,0.82), (0.2,0.65,0.45), (0.03,0.78,0.02), (0.74,0.06,0.89), \\ (0.12,0.26,0.58), (0.28,0.83,0.09), (0.69,0.19,0.31), (0.86,0.37,0.91), \\ (0.37,0.55,0.33), (0.99,0.71,0.12), (0.17,0.34,0.77), (0.46,0.96,0.98).$$

are shown in Figure 3.1.

Table 3.4 describes the numerical accuracy for an exact solution being a sum of random Gaussians given by (3.6).

The numerical results demonstrate that for a nonhomogeneous equation the method gives a very high accuracy ( $10^{-7} - 10^{-9}$  was obtained with only 16 grid points in each direction) and there is also indication of quick convergence to the exact

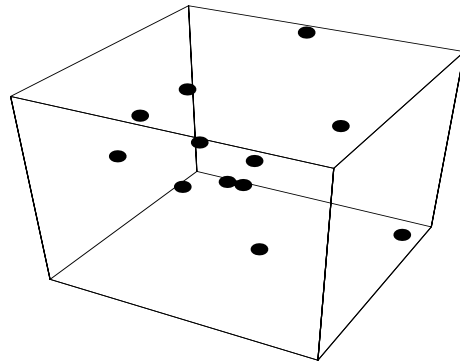


FIG. 3.1. The centers of the Gaussians.

TABLE 3.4

Numerical accuracy for the exact solution being a sum of random Gaussians given by (3.6).

$N_x \times N_y \times N_z$	Number fold. points	$\epsilon_{MAX}$	$\epsilon_{MSQ}$	$\epsilon_{L^2}$
$8 \times 8 \times 8$	4	8.1e-4	8.6e-5	3.0e-5
$16 \times 16 \times 16$	8	7.5e-8	4.4e-9	1.5e-9
$32 \times 32 \times 32$	16	4.4e-9	1.0e-10	3.4e-11

TABLE 3.5

Dependence of the numerical accuracy on the number of grid points and the steepness of the Gaussian for the oscillatory Helmholtz equation with the exact solution given by (3.7), where  $k = 1$ .

$\alpha$	$N_x \times N_y \times N_z$	Number of fold. points	$\epsilon_{MAX}$	$\epsilon_{MSQ}$	$\epsilon_{L^2}$
0.5	$8 \times 8 \times 8$	4	2.0e-6	1.3e-7	1.2e-6
	$16 \times 16 \times 16$	8	5.5e-9	3.5e-10	3.3e-9
	$32 \times 32 \times 32$	16	4.8e-10	1.8e-11	1.8e-10
3	$8 \times 8 \times 8$	4	3.7e-6	1.6e-6	3.3e-6
	$16 \times 16 \times 16$	8	3.4e-8	5.1e-9	1.0e-8
	$32 \times 32 \times 32$	16	7.9e-9	6.4e-10	1.2e-9
15	$8 \times 8 \times 8$	4	2.8e-6	4.2e-7	2.7e-6
	$16 \times 16 \times 16$	8	1.7e-12	4.9e-13	2.9e-12
	$32 \times 32 \times 32$	16	6.6e-14	5.3e-15	3.0e-14
50	$8 \times 8 \times 8$	4	2.5e-2	1.2e-3	1.9e-2
	$16 \times 16 \times 16$	8	2.6e-7	1.6e-8	2.3e-7
	$32 \times 32 \times 32$	16	5.6e-16	4.8e-17	6.7e-16

solution. Tables 3.3 and 3.4 show that the high accuracy is preserved even when the exact solution is very steep near the boundary.

**3.3.2. Oscillatory Helmholtz equation.**

*Example 7.* The right-hand side corresponds to the exact solution

$$(3.7) \quad \Psi(x, y, z) = \exp \left\{ -\alpha \left( (x - 0.5)^2 + (y - 0.5)^2 + (z - 0.5)^2 \right) \right\},$$

where  $k = 1$ .

Table 3.5 illustrates the dependence of the numerical accuracy on the number of grid points and the steepness of the Gaussian for the oscillatory Helmholtz equation given by (3.7).

*Example 8.* Let the right-hand side correspond to the same exact solution as in Example 6 (the sum of random Gaussians), where the equation is the oscillatory

TABLE 3.6

The numerical accuracy for the exact solution of the oscillatory Helmholtz equation being a sum of random Gaussians, where  $k = 1$ .

$N_x \times N_y \times N_z$	Number of fold. points	$\varepsilon_{MAX}$	$\varepsilon_{MSQ}$	$\varepsilon_{L^2}$
$8 \times 8 \times 8$	4	8.1e-4	8.7e-5	3.0e-5
$16 \times 16 \times 16$	8	2.9e-6	3.7e-7	1.3e-7
$32 \times 32 \times 32$	16	7.0e-7	5.0e-8	1.7e-8

Helmholtz equation with  $k = 1$ . The numerical accuracy for the exact solution of the oscillatory Helmholtz equation is given in Table 3.6.

**4. Neumann/mixed problem for the Laplace equation.** Consider the mixed problem for the Laplace equation with Dirichlet boundary conditions at two parallel faces and Neumann boundary conditions on the other faces:

$$(4.1) \quad \Delta \Psi = 0,$$

$$(4.2) \quad \begin{aligned} \frac{\partial \Psi}{\partial z}(x, y, 0+) = f_1(x, y), \quad \frac{\partial \Psi}{\partial z}(x, y, \pi-) = f_2(x, y), \\ \frac{\partial \Psi}{\partial y}(x, 0+, z) = f_3(x, z), \quad \frac{\partial \Psi}{\partial y}(x, \pi-, z) = f_4(x, y), \end{aligned}$$

$$(4.3) \quad \Psi(0+, y, z) = f_5(y, z), \Psi(\pi-, y, z) = f_6(y, z).$$

Suppose that the above six functions are decomposed into sine/cosine series such as

$$(4.4) \quad f_1(x, y) \sim \sum_{m=1, n=0}^{\infty} C_{mn} \sin mx \cos ny, \quad f_5(y, z) \sim \sum_{m, n=0}^{\infty} D_{mn} \cos my \cos nz$$

(sine is for  $x$  while cosine is for  $y, z$ ).

Then the solution of the mixed problem

$$(4.5) \quad \frac{\partial \Psi}{\partial z}(x, y, 0+) = f_1(x, y), \frac{\partial \Psi}{\partial z}(x, y, \pi-) = \frac{\partial \Psi}{\partial z}(x, 0+, z) = \frac{\partial \Psi}{\partial y}(x, \pi-, z) = 0,$$

$$(4.6) \quad \Psi(0+, y, z) = 0, \Psi(\pi-, y, z) = 0,$$

can be presented by the following series

$$(4.7) \quad \sum_{m=1, n=0}^{\infty} C_{mn} \sin mx \cos ny \frac{\cosh \delta_{mn}(\pi - z)}{\delta_{mn} \sinh \delta_{mn} \pi},$$

where  $\delta_{mn} = \sqrt{m^2 + n^2}$ .

The solution with the nonvanishing Dirichlet boundary condition

$$(4.8) \quad \frac{\partial \Psi}{\partial z}(x, y, 0+) = 0, \frac{\partial \Psi}{\partial z}(x, y, \pi-) = 0, \frac{\partial \Psi}{\partial y}(x, 0+, z) = 0, \frac{\partial \Psi}{\partial y}(x, \pi-, z) = 0,$$

$$(4.9) \quad \Psi(0+, y, z) = f_5(y, z), \Psi(\pi-, y, z) = 0,$$

is as follows:

$$(4.10) \quad \sum_{m,n=0}^{\infty} D_{mn} \cos my \cos nz \frac{\sinh \delta_{mn}(\pi - x)}{\sinh \delta_{mn}\pi}$$

with the same  $\delta_{mn}$ .

By adding solutions of the six boundary problems we obtain the solution for the original mixed problem. This series converges quickly if the derivatives in the  $y$  and  $z$  directions vanish on the edges parallel to the  $z$  and  $y$  axes, respectively. To achieve a high-order accuracy we have to treat the first odd derivatives in the same way as even derivatives in the case of the Dirichlet problem. However, here we consider the simplest case corresponding to one subtraction step. At the edges parallel to the  $x$  axis the mixed derivative in  $y$  and  $z$  has to vanish to ensure fast convergence of the cosine series. This is achieved by the procedure which subtracts “edge” functions similar to the one described in section 2.2.

In the case of the mixed problem (4.1)–(4.3) the edge functions have to be modified as follows.

Suppose the function  $f_1(\pi, y)$  can be presented as

$$(4.11) \quad f_1(\pi, y) \sim \sum_{i=0}^{\infty} d_n \cos ny.$$

After subtracting the function

$$(4.12) \quad \sum_{i=0}^{\infty} d_n \cos ny \frac{\cosh \lambda_{1n}(\pi - z)}{\lambda_{1n} \sinh(\lambda_{1n}\pi)} \frac{\sinh(\lambda_{2n}x)}{\sinh(\lambda_{2n}\pi)}, \quad \lambda_{1n}^2 + \lambda_{2n}^2 = n^2,$$

we obtain a solution with the vanishing  $z$ -derivative on  $(\pi, y, 0)$ -edge.

Now let  $g(x, y) = \frac{\partial f_1(x, y)}{\partial y}$  and the decomposition of  $g(x, \pi)$  into the sine series be the following:

$$(4.13) \quad g(x, \pi) \sim \sum_{i=0}^{\infty} d_n \cos ny.$$

Then by subtracting the function

$$(4.14) \quad \sum_{i=1}^{\infty} d_n \sin nx \frac{\cosh \lambda_{1n}y}{\lambda_{1n} \sinh(\lambda_{1n}\pi)} \frac{\cosh(\lambda_{2n}(\pi - z))}{\lambda_{2n} \sinh(\lambda_{2n}\pi)}, \quad \lambda_{1n}^2 + \lambda_{2n}^2 = n^2,$$

we eliminate the mixed  $yz$ -derivative at  $(x, \pi, 0)$ -edges. The other edges are treated similarly.

It is easy to check that the above sine and cosine series for the edges converge quickly if the mixed  $yz$  derivatives of the solution vanish in the corners. Thus, first we subtract the “corner” functions. Let

$$A = \frac{\partial f_1}{\partial y}(0, \pi) = \frac{\partial^2 \Psi}{\partial y \partial z}(0+, \pi-, 0+).$$

Then, for instance, the corner function

$$(4.15) \quad C_{(0,0,\pi)}(x, y, z) = \frac{\sinh(\lambda_1(\pi - x))}{\sinh(\lambda_1\pi)} \frac{\cosh(\lambda_2(\pi - y))}{\lambda_2 \sinh(\lambda_2\pi)} \frac{\cos(\lambda_3 z)}{\lambda_3 \sin(\lambda_3\pi)},$$

TABLE 4.1

The numerical results for the solution (4.16) of the mixed problem using one subtraction step.

$N_x \times N_y \times N_z$	$\varepsilon_{MAX}$	$\varepsilon_{MSQ}$	$\varepsilon_{\mathcal{L}^2}$
$8 \times 8 \times 8$	6.4e-5	8e-6	1.4e-5
$16 \times 16 \times 16$	1.0e-5	6.0e-7	1.0e-6
$32 \times 32 \times 32$	1.7e-6	4.0e-8	7.0e-8
$64 \times 64 \times 64$	2.4e-7	2.7e-9	4.6e-9
$128 \times 128 \times 128$	3.1e-8	1.8e-10	3.0e-10

TABLE 4.2

The numerical results for the solution (4.16) of the Dirichlet problem for the Laplace equation problem using one subtraction step.

$N_x \times N_y \times N_z$	$\varepsilon_{MAX}$	$\varepsilon_{MSQ}$	$\varepsilon_{\mathcal{L}^2}$
$8 \times 8 \times 8$	1.3e-5	1.8e-6	3.0e-6
$16 \times 16 \times 16$	3.5e-6	2.3e-7	4.0e-7
$32 \times 32 \times 32$	9.3e-7	3.1e-8	5.2e-8
$64 \times 64 \times 64$	2.4e-7	3.9e-9	6.7e-9

$\lambda_1^2 + \lambda_2^2 = \lambda_3^2$  has the same mixed  $yz$ -derivative at  $(0, 0, \pi)$ -corner. The arguments can be modified to fit the other corners.

This algorithm is expected to have the same rate of convergence as the corresponding one for the Dirichlet problem with one subtraction step. The only difference is the necessity of having multiple computations of the first derivatives. The accuracy of this operation essentially influences the accuracy of the numerical result. However, if a stencil for computing a derivative contains enough points, then the same convergence as in the Dirichlet case can be achieved, as the following example shows.

*Example 9.* We solve the Laplace equation with Neumann boundary conditions on the XY and XZ faces and Dirichlet boundary conditions on the YZ-face corresponding to the exact solution

$$(4.16) \quad \frac{1}{\sqrt{(x+0.5)^2 + (y+0.5)^2 + (z+0.5)^2}}.$$

Table 4.1 brings the numerical results for the solution of the Laplace equation using one subtraction step.

Here the first derivative was computed by the divided differences method using three grid points.

Table 4.2 gives the results for the same exact solution (4.16) when the Dirichlet problem was solved instead of the mixed one. We observe that the same rate of convergence and similar accuracies were obtained.

**Appendix.** In order to convert the extended function into a function vanishing together with some even derivatives we introduce the bell function  $B(x)$ , supported on the extended interval  $a_1 < a < b < b_1$ :

$$(A.1) \quad \begin{aligned} B^2(x) + B^2(2\bar{a} - x) &= 1, & x \in [a_1, a], \\ B(x) &= 1, & x \in [a, b], \\ B^2(x) + B^2(2\bar{b} - x) &= 1, & x \in [b, b_1], \\ B(x) &= 0, & x < a_1, x > b_1, \end{aligned}$$

where  $\bar{a} = (a + a_1)/2$ ,  $\bar{b} = (b + b_1)/2$ . This function is equal to  $B = 1$  inside the subdomain and smoothly decays outwards over the distance  $2\epsilon = b_1 - b = a - a_1$ . Some particular forms of  $B(x)$  were tested by Israeli, Vozovoi, and Averbuch [11].

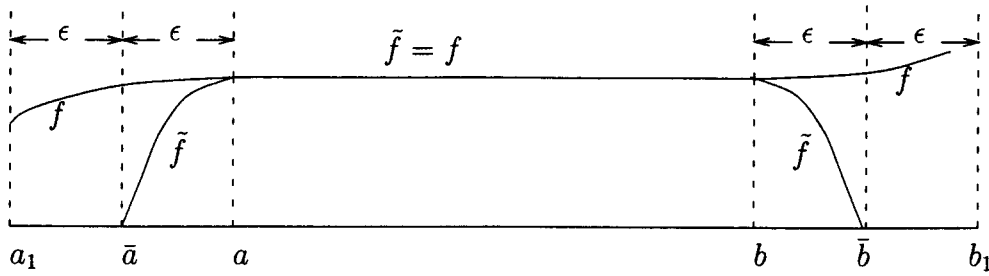


FIG. A.1. The folding operation.

The smoothing of the function  $f$ , denoted by  $\tilde{f}$ , appears as a “folding” across the lines  $\bar{a}$  and  $\bar{b}$ ,  $\tilde{f} \equiv B \cdot f$  (see Figure A.1):

$$(A.2) \quad \tilde{f} = \mathcal{F}_{\bar{a}} \mathcal{F}_{\bar{b}} f(x) = B(x)f(x) - B(2\bar{a} - x)f(2\bar{a} - x) - B(2\bar{b} - x)f(2\bar{b} - x)$$

(the “folded” function  $\tilde{f}$  is defined in  $[\bar{a}, \bar{b}]$ ; the second term is “switched on” only in the interval  $x \in [a_1, a]$  and the third term in the interval  $x \in [b, b_1]$ , respectively). The extra pieces of the function  $f$ , required for the smoothing operation, are provided by overlapping the neighboring subdomains over the  $4\epsilon$  range. On the interval  $x \in [a, b]$  we have  $\tilde{f} = f$ .

The smoothing procedure keeps the function  $\tilde{f}$  highly continuous at  $x = a, b$ . In addition, (A.2) yields that in the vicinity of the points  $x = \bar{a}$ ,  $x = \bar{b}$  the function  $\tilde{f}(x)$  is odd and thus all even derivatives  $\tilde{f}^{(2r)}(\bar{a}) = \tilde{f}^{(2r)}(\bar{b}) = 0$  for  $r = 0, 1, \dots$ . After an antisymmetric reflection across the point  $x = \bar{b}$  (or  $x = \bar{a}$ ) is performed, we obtain a smooth periodic function, which can be represented by a rapidly converging sine series.

In the numerical implementations of the algorithm in this paper the following bell was used:

$$(A.3) \quad B(x) = \begin{cases} 0, & x < a_1 \text{ or } x > b_1, \\ \sin(\theta(x)), & x \in [a_1, a], \\ 1, & x \in [a, b], \\ \cos(\theta(x)), & x \in [b, b_1]. \end{cases}$$

REFERENCES

- [1] G. AHARONI, A. AVERBUCH, R. COIFMAN, AND M. ISRAELI, *Local cosine transform—a method for the reduction of the blocking effect in JPEG*, J. Math. Imaging Vision, 3 (1993), pp. 7–38.
- [2] A. AVERBUCH, M. ISRAELI, AND L. VOZOVoi, *A fast Poisson solver of arbitrary order accuracy in rectangular regions*, SIAM J. Sci. Comput., 19 (1998), pp. 933–952.
- [3] A. AVERBUCH, M. ISRAELI, AND L. VOZOVoi, *On fast direct elliptic solver by modified Fourier method*, Numer. Algorithms, 15 (1997), pp. 287–313.
- [4] E. BRAVERMAN, M. ISRAELI, A. AVERBUCH, AND L. VOZOVoi, *A fast 3D Poisson solver of arbitrary order accuracy*, J. Comput. Phys., 144 (1998), pp. 109–136.
- [5] L. GREENGARD AND J.-Y. LEE, *A direct adaptive Poisson solver of arbitrary order accuracy*, J. Comput. Phys., 125 (1996), pp. 415–424.
- [6] L. GREENGARD AND V. ROKHLIN, *A fast algorithm for particle simulations*, J. Comput. Phys., 73 (1978), pp. 325–348.

- [7] D. GOTTLIEB AND S. A. ORSZAG, *Numerical Analysis of Spectral Methods: Theory and Applications*, SIAM, Philadelphia, 1977.
- [8] D. GOTTLIEB, C. W. SHU, A. SOLOMONOFF, AND H. VANDEVON, *On the Gibbs phenomenon I: Recovering exponential accuracy from the Fourier partial sum of a non-periodic analytic function*, *J. Comput. Appl. Math.*, 43 (1992), pp. 81–92.
- [9] D. GOTTLIEB AND C. W. SHU, *On the Gibbs phenomenon V: Recovering exponential accuracy from collocation point values of a piecewise analytic function*, *Numer. Math.*, 33 (1996), pp. 280–290.
- [10] M. ISRAELI, L. VOZOVoi, AND A. AVERBUCH, *Spectral multi-domain technique with local Fourier basis*, *J. Sci. Comput.*, 8 (1993), pp. 135–149.
- [11] M. ISRAELI, L. VOZOVoi, AND A. AVERBUCH, *Domain decomposition methods for solving parabolic PDEs on multiprocessors*, *Appl. Numer. Math.*, 12 (1993), pp. 193–212.
- [12] G. SKÖLLERMO, *A Fourier method for the numerical solution of Poisson's equation*, *Math. Comput.*, 29 (1975), pp. 697–711.
- [13] L. VOZOVoi, M. ISRAELI, AND A. AVERBUCH, *Spectral multi-domain technique with local Fourier basis II: Decomposition into cells*, *J. Sci. Comput.*, 9 (1994), pp. 311–326.
- [14] L. VOZOVoi, A. WEILL, AND M. ISRAELI, *Spectrally accurate solution of nonperiodic differential equations by the Fourier–Gegenbauer method*, *SIAM J. Numer. Anal.*, 34 (1997), pp. 1451–1471.